Leadership in Sustainable Infrastructure
Leadership en Infrastructures Durables

Vancouver, Canada
May 31 – June 3, 2017/ *Mai 31 – Juin 3, 2017*

BUCKLING RESISTANCE OF STAINLESS STEEL WELDED I-COLUMNS

Ahmed, Shameem [1, 4], Anwar-Us-Saadat, Mohammad [2] and Ashraf, Mahmud [3]
[1,2,3] The University of New South Wales, Australia
[4] Shameem.Ahmed@student.adfa.edu.au

Abstract: Stainless steel is characterised by its nonlinear stress-strain behaviour with significant strain hardening. However, currently available design codes treat it as elastic and perfectly plastic material like carbon steel, which leads to conservative predictions. A new design approach called the Continuous Strength Method (CSM) has recently been developed for nonlinear metallic materials to exploit the beneficial effect of strain hardening and to eliminate the effective width approach. Recently a proposal was made to calculate the buckling capacity of rectangular hollow sections (RHS) and square hollow sections (SHS) combining CSM with Perry curves. In this paper, that proposal is extended for welded I-section. Using finite element technique the behaviour of welded I-section was investigated for major and minor axis buckling. It is observed that, behaviour of column buckling about major axis is different from that of minor axis buckling and required separate column curves. It is also found that, cross section slenderness λ_p has a significant effect on column capacity. The shapes of column curves are mostly affected by λ_p. Hence imperfection factor η, as used in Perry formulations, is expressed as a sigmoidal function where coefficients of the sigmoidal function were expressed as a function of λ_p. This technique yields separate column curves for different λ_p values. Different functions for the coefficients are proposed for major and minor axis buckling. Performance of the proposed technique is compared with European guidelines.

1 INTRODUCTION

Stainless steel is a promising material in the construction industry due to its obvious beneficial properties such as corrosion resistance, aesthetics and negligible maintenance cost. Its stress-strain behaviour is non-linear in nature with no definite yield point. It has significant strain hardening strength. However, current design codes(EN 1993-1-4 2006, SEI/ASCE8-02 2002, AS/NZS 4673 2001) treat stainless steel like carbon steel ignoring its non-linear behaviour and not utilizing its strain hardening benefits. For non-linear metallic material like stainless steel, the Continuous Strength Method (CSM)(Gardner and Nethercot 2004, Ashraf, Gardner, and Nethercot 2006) was evolved. CSM is a strain based design method that incorporates material nonlinearity, exploits strain hardening and incorporates element interactions in predicting resistances at the cross-section level. With the recent development of CSM (Afshan and Gardner 2013, Ahmed, Ashraf, and Anwar-Us-Saadat 2016) cross-section capacity for both stocky and slender cross-section can be predicted through simple formulas with simplified bilinear material model and without calculating the effective area. Therefore, there is scope to use the CSM formulas for prediction the buckling capacity of compression member.

The buckling resistance of stainless steel columns are normally calculated through two different approaches: tangential stiffness method and Perry formulations. SEI/ASCE8-02 (2002) and AS/NZS 4673 (2001) codes use the tangential stiffness method that is an iterative process. In the tangential stiffness method, material nonlinearity is considered through instantaneous tangent modulus but there is no provision for considering imperfection of the member and this method is not applicable for welded sections.

On the other hand, Eurocode (EN 1993-1-4 2006) adapted Perry curves. This is a direct method specifying separate curves for different types of cross-sections based on imperfection parameter. However, Perry curves do not incorporate the material non-linearity. Through numerical analysis, Rasmussen and Rondal (1997) showed that different column curves are necessary to predict the buckling resistance of different grades of stainless steel as their nonlinearity varies a lot from grade to grade. Hradil, Fülöp, and Talja (2012) tried to include the material non linearity in Perry curves by defining transformed slenderness and but their procedure was iterative as they used tangent modulus. Shu, Zheng, and Xin (2014) proposed two base curves and some complicated transfer formulas which could be used to develop multiple curves from two base curves to cover different grades of stainless steel. All of the aforementioned methods use the effective area for slender cross-sections. Huang and Young (2013) proposed a method using full cross section area and material property measured by stub column test to predict the column capacity. Recently Ahmed and Ashraf (2017) proposed new buckling formulas for stainless steel hollow sections based on Perry curves and buckling stress of CSM.

The aim of the current study is to develop a simple design method to determine the buckling resistance of stainless steel welded I-section columns that can explore all the benefits of stainless steel. For this, finite element (FE) models were developed and verified with test results. The verified model was used to identify the influential parameters affecting the column curves through a parametric study. Later FE results were used to develop Perry type column curves for welded I-section based on CSM design principles. Finally, the predictions of the newly proposed formulas were compared with FF results and predictions of other codes.

2 CURRENT DESIGN METHODS FOR BUCKLING RESISTANCE

The tangential stiffness method and Perry-Robertson formulations are two widely used methods to determine the buckling resistance of steel columns. Like carbon steel, the Perry type equations were adopted in Eurocode (EC3) (EN 1993-1-4 2006) for stainless steel columns. Buckling equations currently used in EC3 are presented in Eq. 1 to 5, where A_g is the gross cross-sectional area, f_y is the 0.2% proof stress ($\sigma_{0.2}$), χ is the buckling reduction factor, A_{eff} is the effective cross-sectional area, λ is the non-dimensional slenderness of the column and N_{cr} is the elastic buckling load of the column based on gross area. Effective cross-section properties are used to deal with the local buckling of slender cross-sections of class 4. Four column curves were proposed for different cross-section and loading types and they differ from each other by varying a linear function of imperfection parameter η. The suggested imperfection parameter η is expressed using the relationship, $\eta = \alpha(\lambda - \lambda_0)$ where α and λ_0 factors vary depending on cross-section types. The effect of residual stress of the welded section is also included in η. Stainless steel is a highly nonlinear material and its nonlinearity significantly varies from grade to grade. Rasmussen and Rondal (1997) and Ahmed and Ashraf (2017) showed that these nonlinearity has a significant effect on column resistance. However, in the current EC3 gridlines the effect of material nonlinearity is not recognised.

Tangential stiffness method is based on Euler formulas. American and Australian codes (SEI/ASCE8-02 2002, AS/NZS 4673 2001), follow the tangential stiffness approach to determine the column resistance. This method involves a simple equation as given in Eq. 6, where F_n is buckling stress. F_n can be calculated by Eq. 7 which requires iteration as F_n and the tangent modulus (E_t) are interdependent. By using E_t, the effect of material nonlinearity of stainless steel is incorporated in the tangential stiffness method. Though member imperfection as well as residual stress have a significant effect on column resistance, they are not considered in this approach. All design codes limit the maximum compression capacity of a section to its squash load ignoring the strain hardening strength of stainless steel.

[1] $N_u = \chi A_g f_y$ for Class 1, 2 and 3 cross-sections

[2] $N_u = \chi A_{eff} f_y$ for Class 4 cross-sections

[3] $\lambda = \sqrt{\frac{A_g f_y}{N_{cr}}}$ for Class 1, 2 and 3 cross-sections

[4] $\lambda = \sqrt{\frac{A_{eff} f_y}{N_{cr}}}$ for Class 4 cross-sections

[5] $\chi = \frac{1}{\phi + \sqrt{\phi^2 - \lambda^2}} \leq 1.0$ where, $\phi = 0.5[1 + \eta + \lambda^2]$ and $\eta = \alpha(\lambda - \lambda_0)$

[6] $N_u = A_{eff} F_n$

[7] $F_n = \frac{\pi^2 E_t}{(KL/r)^2} \leq f_y$

3 THE CONTINUOUS STRENGTH METHOD (CSM)

The Continuous Strength Method (CSM) is a strain based design approach where a base curve relates to the deformation capacity of the section and a material model relates to the deformation capacity with buckling stress. Gardner and Nethercot (2004) first proposed this method. Recently Afshan and Gardner (2013) proposed a new base curve as shown in Eq. 8, where normalized deformation capacity $\varepsilon_{csm}/\varepsilon_y$ was expressed as a function of cross-section slenderness λ_p for stocky sections. They set the limiting cross-section slenderness value as 0.68. Up to this limit the cross-section is considered as stocky section and over this limit the cross-section is considered as slender section. They also proposed to use the elastic buckling capacity of a full cross section to determine λ_p which includes the contributions of element interaction appropriately. Instead of complex Ramberg-Osgood model, they used a simple bi-linear material model, which is able to explore the strain hardening benefit for stocky cross-sections and simplify the calculation process. Having determined the normalised deformation capacity of the cross-section from the design base curve and using the proposed material model, the buckling stress f_{csm} which a cross-section can achieve prior to local buckling can be determined using Eq. 9.

[8] $\frac{\varepsilon_{csm}}{\varepsilon_y} = \frac{0.25}{\lambda_p{}^{3.6}}$ but $\frac{\varepsilon_{csm}}{\varepsilon_y} \leq 15, \frac{0.1\varepsilon_u}{\varepsilon_y}$ for $\lambda_p \leq 0.68$

[9] $f_{csm} = f_y + E_{sh}\varepsilon_y\left(\frac{\varepsilon_{csm}}{\varepsilon_y} - 1\right)$ for $\lambda_p \leq 0.68$

Ahmed, Ashraf, and Anwar-Us-Saadat (2016) introduced a new parameter Equivalent Elastic Deformation Capacity ($\varepsilon_{e,ev}$) to extended the CSM for slender cross-sections. They considered the base curve (Eq. 8) for the full range of cross-section slenderness and developed a relationship between $\varepsilon_{e,ev}$ and ε_{csm} by Eq. 10 where C is a constant and depends on the type of cross-sections (for I-section a=3.05 and b=3.0). For $\lambda_p > 0.68$, the buckling stress f_{csm} can be calculated by multiplying $\varepsilon_{e,ev}$ with the Young's modulus E as shown in Eq. 11.

[10] $\varepsilon_{e,ev} = C\varepsilon_{csm}$ for $\lambda_p > 0.68$, where $C = a\lambda_p{}^b$

[11] $f_{csm} = \varepsilon_{e,ev}E = C\varepsilon_{csm}E$ for $\lambda_p > 0.68$

Recently Ahmed and Ashraf (2017) proposed new buckling formulas for RHS and SHS columns using f_{csm} based on the Perry formulations. In their proposal, buckling resistance of a column may be determined by using the Eq. 12. Non-dimensional column slenderness λ_{csm} may be obtained using the modified definition as shown in Eq. 13, where N_u is the buckling resistance of the member, χ is the reduction factor for buckling as given in Eq. 5, Ag is the gross cross-sectional area, and N_{cr} is the elastic critical buckling capacity of the member based on A_g. They observed that non-dimensional proof stress ($e = f_y/E$), strain hardening exponent n and λp have a significant effect on column curves. They modified λ_{csm} to reduced the effect of e and n and introduced modified non dimensional slenderness λ_m. Modifications of λ_{csm} are shown in Eq. 14, where C is the modification factor for e and C_n is the modification factor for n. The reduction factor of the Perry curves similar to current EC3 was adopted in their study replacing the non-dimensional slenderness λ by λm as given in Eq. 15. They proposed a sigmoidal function of λ_m for the imperfection factor η as shown in Eq 16 where A, B and W are the coefficients of the sigmoidal function. Values of A and B were expressed as functions of λ_p, which produce different column curves for different λ_p values.

[12] $N_u = \chi A_g f_{csm}$

[13] $\lambda_{csm} = \sqrt{\frac{A_g f_{csm}}{N_{cr}}}$

[14] $\lambda_m = \lambda_{csm} + C_e + \frac{5-n}{5} C_n \geq 0$

[15] $\chi = \frac{1}{\phi + \sqrt{\phi^2 - \lambda_m^2}} \leq 1.0$ where, $\phi = 0.5[1 + \eta + \lambda_m^2]$

[16] $\eta = \frac{A}{1+exp^{-(\lambda_m - B)/W}} - 0.25$

4 NUMERICAL MODEL

The Commercial finite element analysis package ABAQUS was used for numerical simulation. Initially, the developed FE models were validated against test results and later verified FE models were used to perform parametric study to identify the influence of different parameters on column resistance. Finally, these FE results were used to propose new column curves.

In the FE model, four-noded doubly curved shell elements with reduced integration were used with mesh sizes not greater than 5 mm along the transverse direction and 15 mm along the longitudinal direction for flanges and web of I-section. The two-stage Ramberg–Osgood (R–O) material model proposed by Rasmussen (2003), with recent modifications proposed by Arrayago, Real, and Gardner (2015), was used in developing the FE models. Basic material properties such as Young's modulus (E), proof stress ($\sigma_{0.2}$) and strain hardening exponent (n) were considered as 200 GPa, 400MPa and 7 respectively. In this study, both local and global geometric imperfections were considered. Eigenvalue analysis was performed and the corresponding elastic buckling mode was used to simulate the distribution of imperfections. The amplitude of local geometric imperfection was considered as d/200 and the amplitude of global imperfection was considered as L/1500, where d was the unsupported width of the flange and L was the length of the column. Membrane residual stresses are developed in I-sections due to welding, which induces tensile stress in the vicinity of the welds with compressive stress away from those regions. Residual stresses were incorporated in the FE model according to the proposal of Yuan, Wang, Shi, et al. (2014), where the maximum tensile stress was taken as $0.8\sigma_{0.2}$.

Columns were considered as pin supported at both ends. All nodes at the bottom and the top ends were coupled with two reference points located at the centroid of the corresponding section. Pin support conditions were applied to those reference points allowing for longitudinal translation at the top. Columns subjected to buckle around major axis were laterally supported at mid height to prevent minor axis buckling. Displacements were applied at the top reference point to simulate column tests.

5 VERIFICATION OF THE FE MODEL

The accuracy of the FE model was verified against ten test results of welded I-section columns reported in Yuan, Wang, Gardner, et al. (2014) and Yang et al. (2016). Among test results, five columns were subjected to major axis buckling and the rest of the columns were tested for minor axis buckling. The comparison of ultimate load (N_u) of FE models with those obtained from tests were shown in Table 1. FE results showed good accuracy in predicting the test results as the average ratios of the ultimate loads obtained from FE models and test results was 1.00 with a coefficient of variation (COV) of 0.08. In Figure 1, full load-deflection responses of FE model of two columns, one buckled about minor axis (I304-432-i) and another buckled about major axis (I304-2000), were compared with test responses and they showed good agreement. Overall comparisons shows that the adopted FE model are capable of predicting the behaviours of welded

I-section stainless steel columns, and could be used to generate additional results for parametric study and to develop column curves.

Table 1: Comparison of FE and test results.

Reference	Specimen Id	N_{FE}/N_{test}
Minor axis buckling(Yuan, Wang, Gardner, et al. 2014)	I304-252-i	0.93
	I304-312-i	0.89
	I304-372-i	0.90
	I304-432-i	1.00
	I304-492-i	1.13
Major axis buckling(Yang et al. 2016)	I304-2000	1.03
	I304-3000	0.97
	I304-3500	0.96
	I304-4000	1.08
	I304-4500	1.08
Average		1.00
COV		0.08

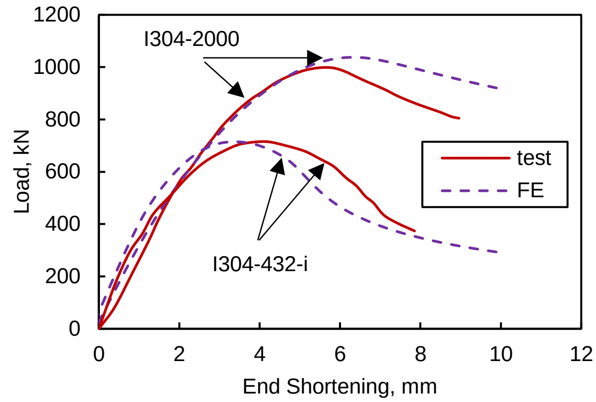

Figure 1: Comparison of load-deformation curves for i-section columns

6 PARAMETRIC STUDY

The verified FE modelling technique was used to identify the parameters that significantly affect the buckling resistance of stainless steel columns through a parametric study. Ahmed and Ashraf (2017) found that cross section slenderness λ_p has a significant effect on column curves of RHS and SHS columns. Therefore, the effect of λ_p on column curves of welded I-section was investigated here. In this study, the effect of other cross-sectional properties like the ratio of width and height (B/H) of the section and the ratio of flange thickness and web thickness (t_f/t_w) were also examined. Both major axis buckling and minor axis buckling were considered here. Three values of B/H vary from 1.0 to 0.5 (1.0, 0.67 and 0.5) and three values of t_f/t_w (1.0, 1.5 and 2.0) were considered to cover a wide range of I-sections. Effects of B/H and t_f/t_w were observed on both stocky and slender cross-sections. Cross section slenderness of stocky section was 0.48 and for slender sections was 0.88. Seven values of cross-section slenderness ranging from 0.39 to 0.98 were considered to evaluate the effect of λ_p on column curves of I-sections. The effect of cross-section slenderness was studied on the cross-sections having B/H = 0.67 and t_f/t_w = 1.5. λ_p was calculated according to the proposal reported in Afshan and Gardner (2013) where the elastic buckling capacity of the full cross section ($\sigma_{cr,cs}$) was determined using CUFSM. A total 23 different I-sections were analysed for major and minor axis buckling and their cross sectional properties are shown in Table 2. For each I-section, columns of 15 different slenderness λ_{csm} (0.2, 0.3, 0.35, 0.4, 0.45, 0.5, 0.55, 0.6, 0.8, 1.0, 1.2, 1.4, 1.6, 1.8 and 2.0) were analyzed to get the full range of column curves. A total of 690 models were analysed to obtain a thorough understanding of buckling behaviour of stainless steel I-section columns.

Table 2: Cross-sectional properties of I-sections

Sl. No.	H (mm)	B (mm)	t_f/t_w (mm/mm)
1-6	150	150	8.05/8.05, 4.54/4.54, 9.0/6.0, 5.1/3.4, 9.45/4.73, 5.47/2.74
7-17	225	150	9.6/9.6, 5.38/5.38, 14.15/9.43, 11.5/7.67, 9.65/6.43, 8.35/5.57, 7.35/4.9, 6.56/4.37, 5.93/3.95, 13.83/6.92, 8.03/4.02
18-23	300	150	12.17/12.17, 6.83/6.83, 15.48/10.32, 8.82/5.88, 19.4/9.7, 11.22/5.61

7 ANALYSIS OF FE RESULTS

To observe the effect of different parameters, column curves are plotted in Figures 2 to 4. In these column curves, non-dimensional column strength or reduction factor χ was calculated as $\frac{N_{u,FE}}{A_g f_{csm}}$. In Figure 2, the influence of λ_p on column curves is shown for major axis buckling and minor axis buckling respectively. It is observed that cross-section slenderness λ_p has a significant effect on column curves of welded I-section and it is similar to the effect observed on the column curves of RHS and SHS (Ahmed and Ashraf 2017). In both cases, column curves move upward with increasing values of λ_p i.e. the reduction factor χ is higher for relatively slender cross-sections with higher value of λ_p. Shapes of column curves also depend on λ_p. For slender cross-sections (with higher value of λ_p), the column resistance approaches to its cross-section capacity i.e. χ approaches 1.00 at a relatively higher value of λ_m when compared against stocky cross-sections (with smaller λp).The effect of λ_p is more prominent at the intermediate portion of column curves and diminishes with the increase of λ_m.

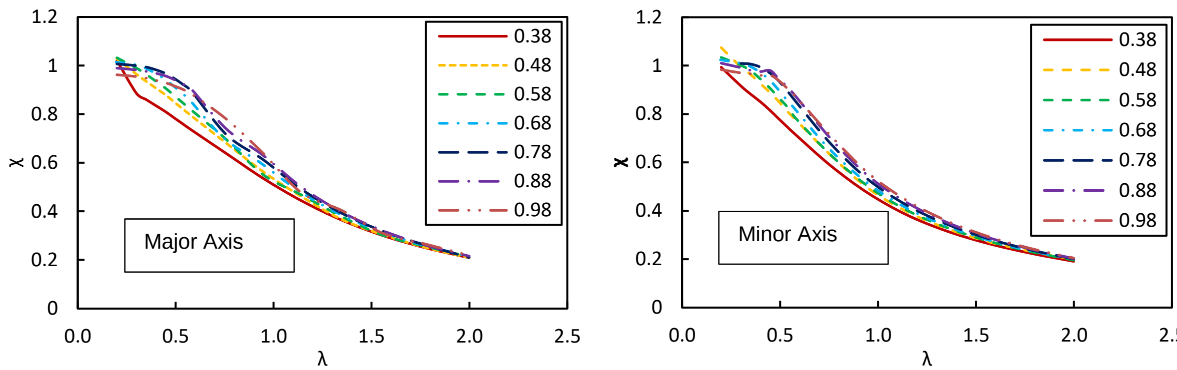

Figure 2: Column curves for buckling of welded I-section for different λ_p values

Figures 3 and 4 show the effect of B/H and t_f/t_w on column curves respectively for both stocky and slender cross-sections. It was observed that B/H and t_f/t_w have no significant effect on column curves of stocky sections (λ_p=0.48). In case of slender sections (λ_p = 0.88), B/H showed some minor effect on column curves at low λ_m values. From Figure 4 and 5 it is also clear that column resistance for major axis buckling is higher than that of minor axis buckling. This effect is more prominent at the intermediate portion of column curves and diminishes with the increase or decrease of λ_m. From this analysis, it is clear that separate column curves are required for major axis buckling and minor axis buckling and the effect of λ_p should be included in the formulas.

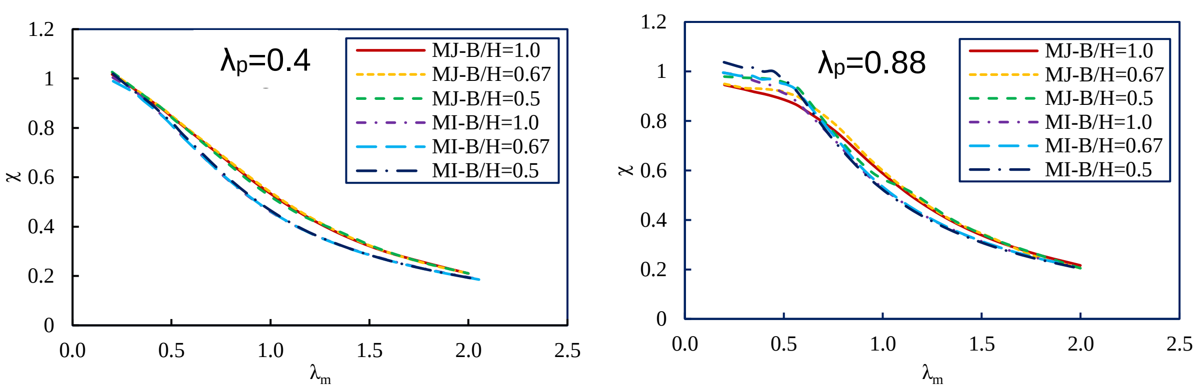

Figure 3: Column curves of welded I-sections for different B/H ratios

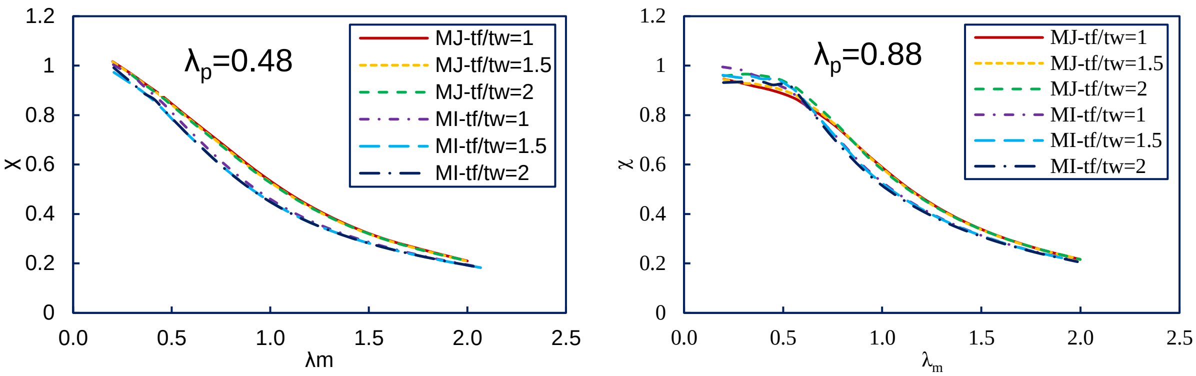

Figure 4: Column curves of welded I-sections for different t_f/t_w ratios

8 IMPERFECTION FACTOR η FOR WELDED I-SECTION

In this study, an attempt was made to predict the buckling capacity of welded I-section columns based on the Perry curves proposed by Ahmed and Ashraf (2017) as given in Eq. 12 to 16. To get an appropriate function of imperfection factor η for I-section, values of η were calculated from the FE results and were plotted against λ_m for different values of λ_p and shown in Figure 5. From this figure, it is clear that like column curves, λ_p has a significant influence on η and the variation of η with λ_m can be well represented by the sigmoidal function of Eq. 16. The coefficients A, B and W of the sigmoidal function were determined for I-sections for both major and minor axis buckling. Value of A and B depend on λ_p. Eq. 17 and 18 gives the value of A and B for major axis buckling and Eq. 19 and 20 gives the values for minor axis buckling. A constant value of W = 0.4 is proposed for both major axis buckling and minor axis buckling.

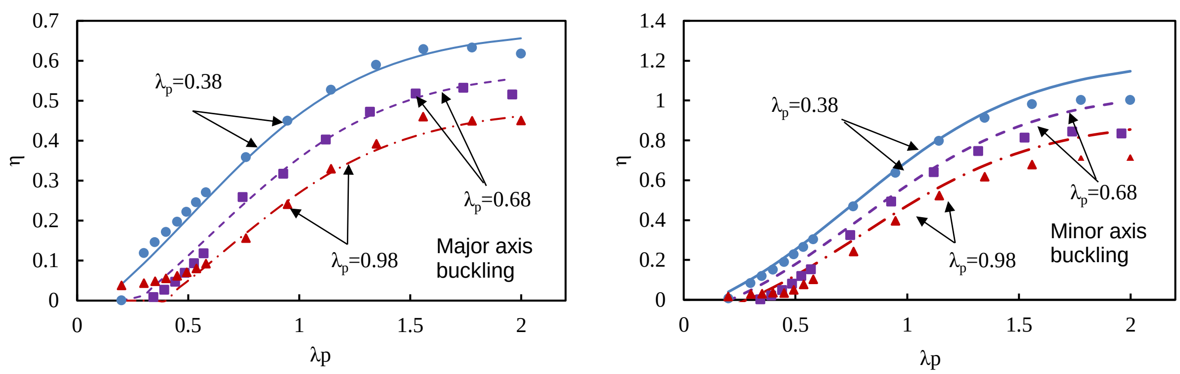

Figure 5: η calculated from FE results and proposed curves of η for different λ_p values

[17] $A = -0.32\lambda_p + 1.55$

[18] $B = 0.3\lambda_p + 0.4 \ \leq 0.65$

[19] $A = -0.5\lambda_p + 1.65$

[20] $B = 0.1\lambda_p + 0.72 \ \leq 0.80$

9 COMPARISON OF THE PROPOSED METHOD

The accuracy of the proposed method was verified with FE results and was compared with EC3. The key features of the comparison are shown in Table 3. It is observed that proposed CSM formula predictions are more accurate and more consistent. For both major axis buckling and minor axis buckling, the average of the ratio of CSM predictions and FE results was 0.98 where these average of EC3 predictions were 0.93 and 0.89 respectively. The coefficient of variation (COV) for CSM predictions is always less than that of EC3 predictions. Figures 6 also illustrates the comparison of CSM predictions and EC3 predictions with FE results. Both the figures show that the performance of CSM formulas is more accurate than EC3 for the full slenderness range.

Table 3: Performance of the proposed CSM technique and EC3

Loading condition	N_{csm}/N_{FE}		N_{EC3}/N_{FE}	
	Average	COV	Average	COV
Major axis buckling	0.99	0.03	0.93	0.04
Minor axis buckling	0.97	0.04	0.89	0.05

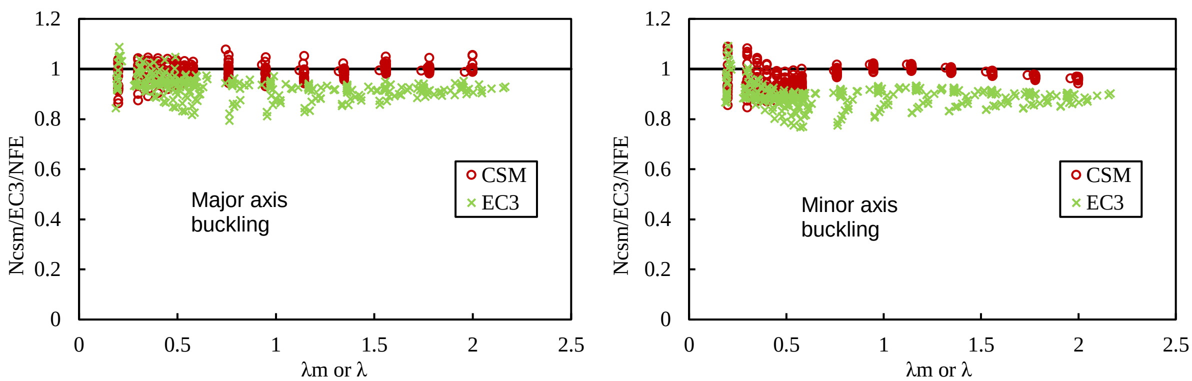

Figure 6: Comparison of CSM and EC3 predictions for major and minor axis buckling

10 CONCLUSION

Currently available design codes of stainless steel do not address its nonlinear material behaviour and do not consider the strain hardening benefits. They also follow the calculation intensive effective width approach for slender cross-sections. In this study, new design formulas for predicting buckling resistance were proposed for welded I-sections. In this proposal, the buckling stress f_{csm} of CSM is used instead of material yield stress in basic Perry curves. A parametric study was performed using verified FE model to observe the effect of cross-section slender, B/H and t_f/t_w . It is found that B/H and t_f/t_w have no significant effect on column curves and can be ignored in the formulation of column curve. However, cross-section slender has a significant effect on column curves of welded I-sections. Hence, the imperfection factor η was expressed as a sigmoidal function of λ_m where the coefficients of that function depend on λ_p. It is also observed that for welded I-section, column curves for major axis buckling are different from that of minor axis buckling. So different equations are proposed for the coefficient A and B for major and minor axis buckling. Due to the use of f_{csm} and gross cross-section area, this new method incorporates the strain hardening benefits and eliminates the effective area calculation. Compare to EC3, this method is simple to use but produced more accurate and more consistent predictions.

References

Afshan, Sheida, and Leroy Gardner. 2013. "The continuous strength method for structural stainless steel design." *Thin-Walled Structures* no. 68:42-49.

Ahmed, Shameem, and Mahmud Ashraf. 2017. "Numerical investigation on buckling resistance of stainless steel hollow members." *Journal of Constructional Steel Research*:under review.

Ahmed, Shameem, Mahmud Ashraf, and Mohammad Anwar-Us-Saadat. 2016. "The Continuous Strength Method for slender stainless steel cross-sections." *Thin-Walled Structures* no. 107:362-376.

Arrayago, I, E Real, and L Gardner. 2015. "Description of stress–strain curves for stainless steel alloys." *Materials & Design* no. 87:540-552.

AS/NZS 4673. 2001. Cold-formed stainless steel structures. Sydney: Standards Australia.

Ashraf, M., L. Gardner, and D. A. Nethercot. 2006. "Compression strength of stainless steel cross-sections." *Journal of Constructional Steel Research* no. 62 (1-2):105-115.

EN 1993-1-4. 2006. Eurocode 3: Design of steel structures – Part 1.4:General rules – supplementary rules for stainless steels. Brussels: European Committee for Standardization (CEN).

Gardner, L., and D. A. Nethercot. 2004. "Experiments on stainless steel hollow sections—Part 1: Material and cross-sectional behaviour." *Journal of Constructional Steel Research* no. 60 (9):1291-1318.

Hradil, Petr, Ludovic Fülöp, and Asko Talja. 2012. "Global stability of thin-walled ferritic stainless steel members." *Thin-Walled Structures* no. 61:106-114.

Huang, Y., and B. Young. 2013. "Tests of pin-ended cold-formed lean duplex stainless steel columns." *Journal of Constructional Steel Research* no. 82:203-215.

Rasmussen, Kim J. R. 2003. "Full-range stress–strain curves for stainless steel alloys." *Journal of Constructional Steel Research* no. 59 (1):47-61.

Rasmussen, KJR, and J Rondal. 1997. "Strength curves for metal columns." *Journal of Structural Engineering* no. 123 (6):721-728.

SEI/ASCE8-02. 2002. Specification for the Design of Cold-Formed Stainless Steel Structural Members. Reston: American Society of Civil Engineers (ASCE).

Shu, Ganping, Baofeng Zheng, and Lianchun Xin. 2014. "A new design method for stainless steel columns subjected to flexural buckling." *Thin-Walled Structures* no. 83:43-51.

Yang, Lu, Menghan Zhao, Tak-Ming Chan, Fan Shang, and Dongchen Xu. 2016. "Flexural buckling of welded austenitic and duplex stainless steel I-section columns." *Journal of Constructional Steel Research* no. 122:339-353.

Yuan, H. X., Y. Q. Wang, L. Gardner, and Y. J. Shi. 2014. "Local–overall interactive buckling of welded stainless steel box section compression members." *Engineering Structures* no. 67 (0):62-76.

Yuan, H. X., Y. Q. Wang, Y. J. Shi, and L. Gardner. 2014. "Residual stress distributions in welded stainless steel sections." *Thin-Walled Structures* no. 79:38-51.